

Lattice dynamics in ZrB_{12} and LuB_{12} : *Ab initio* calculations and inelastic neutron scattering measurements

A. V. Rybina,¹ K. S. Nemkovski,^{1,*} P. A. Alekseev,¹ J.-M. Mignot,² E. S. Clementyev,¹ M. Johnson,³ L. Capogna,³
 A. V. Dukhnenko,⁴ A. B. Lyashenko,⁴ and V. B. Filippov⁴

¹*ISSSPh, RRC “Kurchatov Institute,” Moscow, Russia*

²*Laboratoire Léon Brillouin, CEA-CNRS, CEA/Saclay, Gif sur Yvette, France*

³*Institut Laue-Langevin, Grenoble, France*

⁴*Institute for Problems of Materials Science, NASU, Kiev, Ukraine*

(Received 31 March 2010; revised manuscript received 18 June 2010; published 8 July 2010)

The first *ab initio* calculations using ultrasoft pseudopotentials within the local-density approximation in superconducting ZrB_{12} are reported, together with an inelastic neutron scattering study of its lattice dynamics. As in previously studied rare-earth dodecaborides, the phonon spectra are mainly determined by vibrations of the rigid boron network whereas Zr atoms vibrations have a quasilocal character and are localized in a narrow energy range around $E \approx 17$ meV. The results consistently indicate that the phonon modes corresponding to Zr vibrations are responsible for a considerable electron-phonon interaction and could take part in the formation of the superconducting state below $T_c \approx 6$ K as was suggested previously.

DOI: [10.1103/PhysRevB.82.024302](https://doi.org/10.1103/PhysRevB.82.024302)

PACS number(s): 74.25.Kc, 63.20.dk, 63.20.dd, 78.70.Nx

I. INTRODUCTION

Dodecaborides (MB_{12}) and, to some extent, hexaborides (MB_6) can be regarded as clathratelike¹ cluster compounds, in which boron atoms form a rigid network embedding weakly bound metal atoms. The boron network essentially determines the mechanical properties of the material while the metal sublattice governs its electronic transport and magnetic properties. These systems look rather promising for technical applications owing to their unique combination of valuable properties—high-melting points, hardness, thermal, and chemical stability. Furthermore, they could serve as a paradigm for other cluster compounds such as fullerides or higher borides.² Recent success in growing large high-quality single crystals of dodecaborides renewed the interest in this class of materials and triggered new experimental investigations by a number of techniques. MB_6 and MB_{12} compounds containing divalent ion M^{2+} are insulators whereas those containing M^{3+} and M^{4+} ions are metallic. This can be used in tuning the properties of materials intended for specific applications.

Of particular interest is the superconducting state discovered in the late 1960s by Matthias *et al.*³ in several of these compounds ($M = \text{Sc}, \text{Y}, \text{Zr}, \text{La}, \text{Lu}, \text{and Th}$). ZrB_{12} exhibits the highest $T_c \sim 6$ K among dodecaborides. It was previously suggested⁴ that the superconductivity in YB_6 and ZrB_{12} is directly connected with the vibrations of boron complexes. On the other hand, the much smaller isotope effect on T_c produced by boron, in comparison with Zr, in ZrB_{12} suggests that lattice vibration modes involving Zr atoms play a key role in the electron-phonon coupling responsible for superconductivity.^{5,6} The role of quasilocal Zr vibrations was emphasized recently in a detailed experimental study of the thermal and transport properties of this compound.⁷ However, information on the vibrational spectra in ZrB_{12} is rather scarce. The specific-heat results reported in Ref. 7 have been interpreted as evidence for a pronounced peak, at about 15 meV, in the low-energy phonon density of states (PhDOS),

which was attributed to Zr vibrations.⁷ A sharp phonon peak at similar energies was indeed observed directly in the inelastic neutron scattering (INS) spectra of the related compounds YbB_{12} and LuB_{12} .^{8,9} The contribution of low-energy Zr vibrations to the electron-phonon coupling was also reported from Seebeck effect measurements.¹⁰ In the latter work, the energy of Zr vibrations was estimated to be 18.6 meV. Direct information on phonon energies in ZrB_{12} was so far limited to zone-center frequencies obtained from Raman experiments¹¹ and related mainly to boron vibrations.

In order to single out the peculiarities of electron-phonon interactions in ZrB_{12} and their possible effects on the superconducting properties, we have performed *ab initio* calculations, as well as detailed single-crystal INS measurements of the lattice dynamics in this compound. Previously we had measured the PhDOS (Ref. 12) and phonon-dispersion curves¹³ in the rare-earth dodecaborides YbB_{12} and LuB_{12} , which are isostructural to ZrB_{12} . These measurements clearly showed that the high-energy part of the phonon spectrum (above $E \sim 20$ meV and up to a cutoff energy of about 135 meV) is determined mainly by the vibrations of the rigid boron network. The spectrum of boron vibrations is identical for YbB_{12} and LuB_{12} and thus can be expected to be similar also for other dodecaborides. This is further confirmed by the *ab initio* calculations for ZrB_{12} and LuB_{12} performed in the present work. Therefore, INS experiments were restricted here to the lower energy range ($E \leq 40$ meV) in which the Zr vibration modes, thought to be the most relevant to the superconducting pairing, are located.

II. EXPERIMENTAL DETAILS

A single-crystal sample of ZrB_{12} (volume ~ 0.4 cm³) was prepared by the traveling-solvent melting technique¹⁴ using ¹¹B isotope (99.5% enrichment) at the Institute for Problems of Materials Science in Kiev. Preliminary room-temperature INS experiments were performed on the triple-axis spectrometer ATOS at RRC “Kurchatov Institute” in Moscow.

TABLE I. Comparison of the calculated and experimental lattice parameter a and boron position parameter x for ZrB_{12} and LuB_{12} .

	a (Å)		x	
	Experiment	Calculation	Experiment	Calculation
ZrB_{12}	7.4077	7.415	0.1667	0.1606
LuB_{12}	7.4634	7.458	0.1693	0.1619

The detailed study of phonon dispersions was then carried out on the thermal-beam triple-axis spectrometer 2 T at the Laboratoire Léon Brillouin in Saclay. The sample was oriented with a $\langle 110 \rangle$ crystallographic axis normal to the scattering plane. The spectra were recorded at fixed final neutron energies, with a pyrolytic graphite (PG) 002 ($E_f = 14.7$ meV) or a Cu 111 ($E_f = 30.5$ meV) monochromator, a PG 002 analyzer, and a PG filter inserted in the scattered beam to suppress higher order contaminations. For the TA branches along the $[\xi\xi 0]$ direction we also performed a high-resolution study of the temperature evolution of the phonon dispersion across T_c . The measurements were carried out on the cold-beam triple-axis spectrometer 4F1 (PG 002 monochromator and analyzer, $E_f = 8.0$ meV) in the low-energy region (up to 5 meV) and in the temperature range 2–8 K. The energy resolution at zero energy transfer was 0.4 meV

III. *AB INITIO* CALCULATIONS AND INS RESULTS

Ab initio calculations were performed within the local-density approximation of the density-functional theory, using the VASP package^{15,16} and the PHONON computer code.¹⁷ Ultrasoft pseudopotentials were used as implemented in VASP. The projector-augmented wave pseudopotentials for Zr (Lu) and B atoms represented $4s^2 4p^4 5s^2 4d^4$ ($5s^2 5p^4 6s^2 5d^3 4f^{14}$) and $2s^2 2p^1$ electron configurations, respectively. The wave functions were expanded in plane waves up to a kinetic cutoff of 269.24 eV.

The crystal structure of ZrB_{12} is of UB_{12} type (fcc space group $Fm\bar{3}m$). The lattice parameters obtained from x-ray powder diffraction are 7.4077(9) Å and 7.4634(2) Å for ZrB_{12} and LuB_{12} , respectively. The coordinates of the Zr (Lu) atom in the cubic unit cell are (0, 0, 0) whereas 12 boron atoms occupy the parametric positions $(0.5, 0.5 \pm x, 0.5 \pm x)$, $(0.5 \pm x, 0.5, 0.5 \pm x)$, and $(0.5 \pm x, 0.5 \pm x, 0.5)$ with all possible combinations of plus and minus signs. The values of the position parameter x are listed in Table I. For all calculations the supercell was chosen to be the standard fcc unit cell. It contains four MB_{12} formula units and 52 atoms. The Brillouin zone was sampled by a $4 \times 4 \times 4$ Monkhorst-Pack mesh of k points.¹⁸ The phonon frequencies were determined by the direct method. The Hellmann-Feynman forces were computed for positive and negative atom displacements with an amplitude of 0.03 Å.

The calculation was performed with full structural relaxation. The relevance of this choice is ensured by the good agreement between calculated and experimental values of the lattice (a) and position (x) parameters (Table I) for ZrB_{12} and

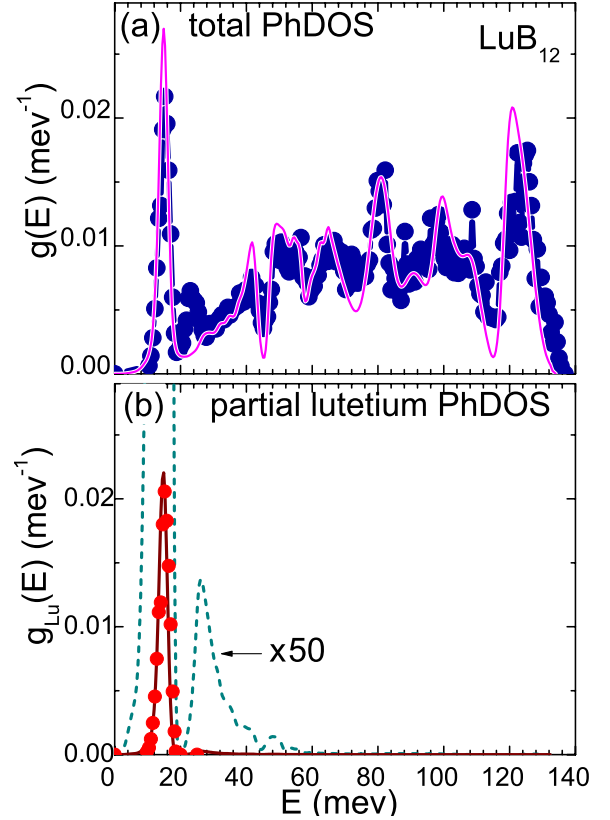


FIG. 1. (Color online) Phonon density of states in LuB_{12} . Symbols: PhDOS refined from the experimental INS spectra (Ref. 12); lines: results of *ab initio* calculation, convoluted with the experimental resolution function. (a) Total PhDOS. (b) Partial lutetium PhDOS. The dashed line represents the same data plotted on an expanded (by a factor of 50) scale.

LuB_{12} . It is also worth noting that the calculation yields smaller values for both a and x in the case of ZrB_{12} , with the correct ratios between the two compounds.

For both ZrB_{12} and LuB_{12} we have calculated the phonon dispersion along three main symmetry directions. The PhDOS was then obtained by averaging the dispersion curves over the Brillouin zone.

In Fig. 1 the calculated PhDOS for LuB_{12} is shown together with the PhDOS refined from the experimental INS spectra (separation of partial contribution and Debye-Waller factors performed self-consistently from experimental data for LuB_{12} and YbB_{12} , in analogy with the isotopic contrast method—see Ref. 12 for details). To help comparison, the calculated PhDOS was convoluted with the experimental resolution function of the time-of-flight spectrometer (HET, ISIS, U.K.) on which the measurements of Ref. 12 were performed. The high-energy part of the PhDOS is determined by boron vibrations. Good agreement is found between the calculation and the experimental data, except for some discrepancy at energies of 20–30 meV, due to the incorrect description of the weakly dispersive optic branch located¹³ in this energy range. This branch gives rise to the peak at about 23 meV in the experimental LuB_{12} PhDOS [Fig. 1(a)] and is related mainly to the boron vibrations, as follows from the comparison of experimental data in Figs. 1(a) and 1(b). The

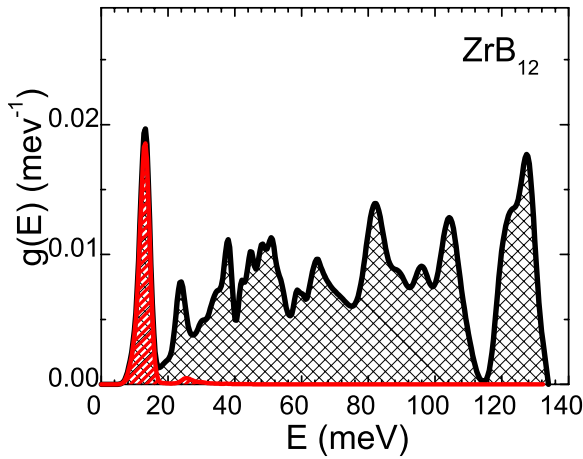


FIG. 2. (Color online) Calculated PhDOS in ZrB₁₂, convoluted with the same resolution function as in Fig. 1. Cross-hatched area: total PhDOS; hatched area: partial zirconium PhDOS.

low-frequency part of the phonon spectrum, below about 20 meV, is mainly related to Lu vibrations. The partial PhDOS for Lu [Fig. 1(b)] is characterized by a strong peak at 15 meV in both the experimental and calculated spectra, and by a very weak peak at about 30 meV in the calculated PhDOS, which cannot be observed within the accuracy of the neutron measurements. The latter peak originates from long-period lutetium vibrations whose energy is enhanced through hybridization with boron branches.

The PhDOS calculated for ZrB₁₂ is displayed in Fig. 2 (for the sake of comparison, the data were convoluted with the same experimental resolution function as was done above for LuB₁₂). The main features were found to be very similar for the two compounds, especially in the region where boron vibrations dominate.

The calculated dispersion curves for the energy region up to 40 meV are plotted in Fig. 3, together with the data points from the neutron experiments. Typical single-crystal INS spectra from which these data were derived are presented in Fig. 4. The energies of the modes were obtained from Gaussian fits to the experimental spectra. The measured acoustic and lower optic modes exhibit the same general trends as those already reported for the rare-earth dodecaborides YbB₁₂ and LuB₁₂,¹³ which are likely common to this whole class of compounds. Longitudinal- and transverse-acoustic branches are almost degenerate and characterized by the existence of large flat regions as the wave vector approaches the Brillouin-zone boundary. The energy of these flat parts is about 17.5 meV, a few millielectronvolts higher than in LuB₁₂.

Basing on the present calculation scheme, we have studied how the electronic density of states responds to the lattice distortions caused by certain particular phonons. This “frozen phonon” approach makes it possible to analyze the contributions of selected phonon branches to the electron-phonon coupling qualitatively. Here the calculation of the electronic density of states was performed for the undisturbed lattice (atoms fixed at their equilibrium point), then after applying atomic displacements corresponding to the maximum amplitude of zero-point oscillations for a given

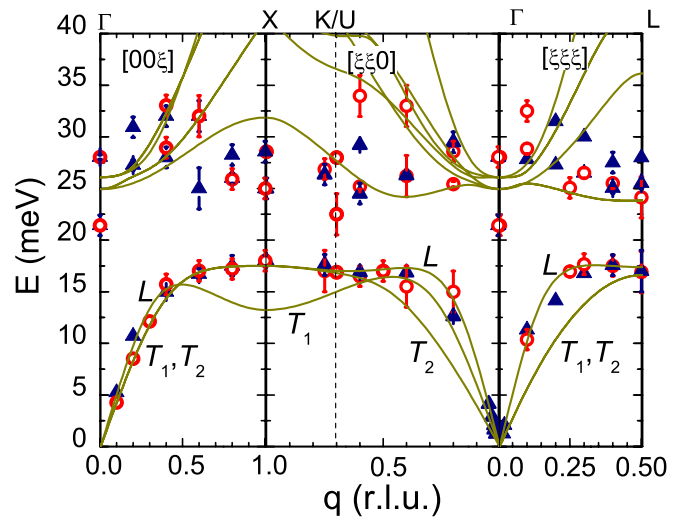


FIG. 3. (Color online) Phonon dispersion in ZrB₁₂ along the main symmetry directions. Lines: *ab initio* calculation. *L* and *T*₁, *T*₂ denote the longitudinal- and transverse-acoustic branches, with *T*₁ having its polarization vectors within the experimental scattering plane, and *T*₂ perpendicular to this plane. Symbols: experiment [circles and triangles correspond to branches measured in the longitudinal and transverse (*T*₁) configurations, respectively].

phonon branch. The results shown in Fig. 5 were obtained for a TA phonon along $[\xi\xi0]$ direction at the Brillouin-zone boundary [*X* point $q=(1,1,0)$, $E=17.5$ meV].

To probe the effects of electron-phonon interactions experimentally, we have checked the temperature evolution of some lattice vibration modes near T_c . Measurements were performed in the energy range 0–5 meV, on the order of the superconducting gap 2Δ , where a softening could occur below T_c . TA branches are more favorable experimentally because transverse phonons are more intense and neutron focusing conditions are easier to achieve. The $[\xi\xi0]$ direction was tentatively selected because the *ab initio* calculation for $q=(1,1,0)$ suggested that this branch could appreciably disturb the electron density of states, and therefore play a sig-

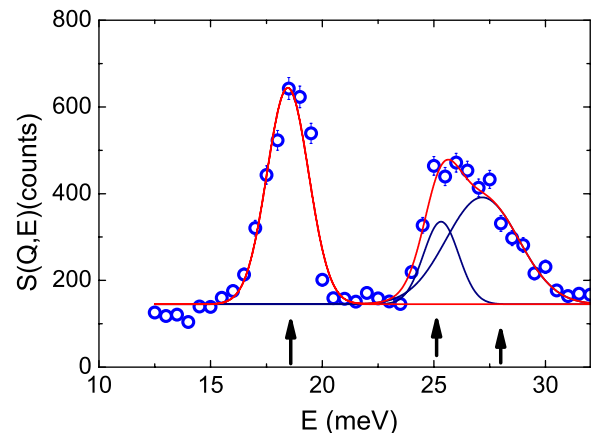


FIG. 4. (Color online) Typical phonon group in ZrB₁₂ measured for $Q=(4.4,1.6,1.6)$ ($[\xi\xi\xi]$ branch) at $T=2.3$ K; counting time was about 5 min per point. The fit by Gaussian functions is shown as solid lines. Arrows indicate the peak positions.

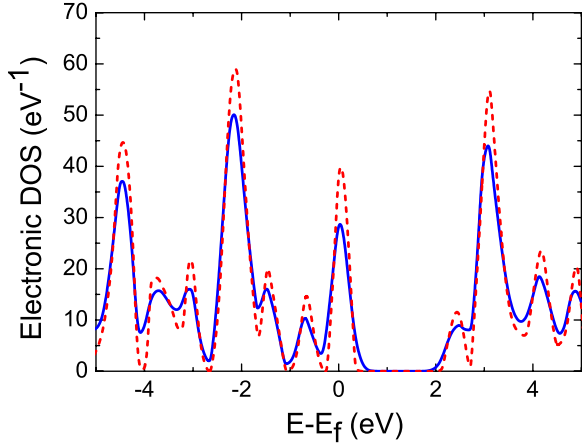


FIG. 5. (Color online) *Ab initio* calculation of the electron density of states in ZrB_{12} for the undisturbed crystal structure (solid line) and in the presence of atomic displacements corresponding to a $\mathbf{q}=(1,1,0)$ transverse phonon with energy $E=17.5$ meV at $T=0$ (dashed line).

nificant role in the electron-phonon interaction. The results obtained below and above the superconducting transition ($T=2$ and 8 K) are presented in Fig. 6. The transition to the superconducting state appears to produce a weak but definite softening for energies around 2 meV, close to the gap value estimated by different methods [2–2.5 meV (Refs. 7 and 19) and references therein].

IV. DISCUSSION

In the previous section, it was shown that, for LuB_{12} , the calculation accounts quite well for the high-energy part ($E \geq 30$ meV) of the boron vibration spectrum as obtained from the INS measurements. It is very likely that the same would also hold true for ZrB_{12} , where the experimental data were restricted to $E \leq 35\text{--}40$ meV. The validity of the calculations performed for both LuB_{12} and ZrB_{12} is further confirmed by the good agreement with the data obtained by Raman spectroscopy (Table II).¹¹

On the other hand, in the low-energy region, which is of particular interest with respect to electron-phonon interactions, the model fails to correctly describe the experimental dispersion of acoustic and lower optic phonons. In particular, in Fig. 3 one notes a sizable disagreement between the ex-

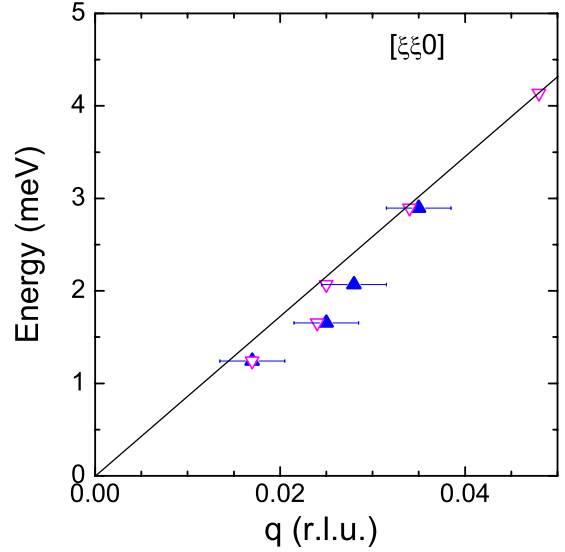


FIG. 6. (Color online) Temperature dependence of the acoustic mode (center of peak) along the $[\xi\xi 0]$ direction close to the Brillouin-zone center. Closed triangles: $T=2$ K and open inverted triangles: $T=8$ K.

perimental and calculated dispersions for the LA branch along $[00\xi]$ and the TA branch T_1 along $[\xi\xi 0]$. The calculated dispersion has a well-pronounced minimum near the zone boundary X point, which is not observed experimentally. This disagreement may indicate that the interaction between Zr ions introduced in the pseudopotential method is too large.

The discrepancy between the calculation and the experiment for the TA branch along $[\xi\xi\xi]$ observed at small q values may have a different origin: since the size of the supercell used in *ab initio* calculation is finite, the calculation may fail to correctly describe the slope of the acoustic branches in the long-wavelength limit. It is indeed found that the sound velocities derived from the *ab initio* calculation are slightly underestimated in comparison with the values obtained from the ultrasonic measurements.²⁰ This effect exists for *all* directions but appears to be most pronounced along $[\xi\xi\xi]$ and for the T_2 branch along $[\xi\xi 0]$ (which was not measured in the present experiment).

In order to model the experimental low-energy lattice dynamics more consistently for all three compounds, we have applied to ZrB_{12} the same simple phenomenological force-

TABLE II. Energies of the Raman-active phonon modes at the Brillouin-zone center for ZrB_{12} and LuB_{12} . Experimental values are taken from Ref. 11.

		E ($\text{cm}^{-1}/\text{meV}$)			
Phonon symmetry		E_g	F_{2g}	E_g	A_{1g}
ZrB_{12}	Calculation	628/77.9	803/100.0	1017/126.1	1086/134.6
	Experiment	642/80.0	796/98.7	1012/125.5	1090/135.1
LuB_{12}	Calculation	625/77.5	779/96.6	995/123.4	1042/129.23
	Experiment	663/82.2	784/97.2	1015/125.8	1043/129.3

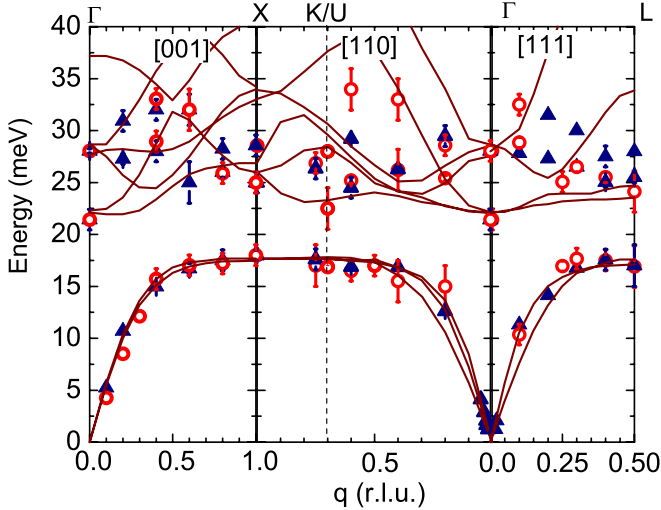


FIG. 7. (Color online) Low-energy phonon dispersion in ZrB_{12} for high-symmetry directions. Symbols: experiment [circles and triangles correspond to branches measured in the longitudinal and transverse (T_1) configurations, respectively]. Lines: force-constant calculation derived from the model of Ref. 13 for LuB_{12} by taking into account the difference in atomic masses and adjusting the Zr-Zr and Zr-B interactions.

constant model used previously for YbB_{12} and LuB_{12} .¹³ The calculations were performed using the UNISOFT software package.²¹ From both the experimental data^{12,13} and the results of the above calculations, it was assumed that the interaction between boron atoms in ZrB_{12} is the same as in the other two systems. Taking into account the difference between Zr and Lu atomic masses, the dispersions for the acoustic and low-energy optic branches were reproduced correctly by adjusting the Zr-Zr and Zr-B interactions (see Fig. 7). The corresponding force constants are listed in Table III, together with similar data for LuB_{12} . The force constant for the B-B interaction (nine coordination spheres) was of order of 10–100 N/m (a comprehensive list is given in Ref. 13).

The phenomenological model thus provides reliable information on the interactions between the Zr atom and its surroundings. In particular, the results indicate that the vibrations of the metal atoms in ZrB_{12} can be considered quasilocal, as was supposed in Ref. 7. The energy of these quasilocal modes was estimated from the flat part of acoustic branches to be about 17.5 meV. This result obtained directly from a spectroscopic probe is consistent with that derived previously from specific-heat and transport measurements.^{7,10} One notes, however, that the value for ZrB_{12} is closer to those obtained for YbB_{12} and LuB_{12} than could be expected from the ratio of masses between zirconium and the rare earths (21 meV). This discrepancy is thought to result from the change in interatomic M - M and M -B interactions upon substituting Zr^{4+} for Lu^{3+} .

Although the *ab initio* calculations do not yield a quantitative description of acoustic-phonon dispersion, they pro-

TABLE III. Comparison of force-constant parameters for LuB_{12} and ZrB_{12} .

Interaction	Force-constant parameters (N/m)			
	First coordination sphere		Second coordination sphere	
	Longitudinal	Transverse	Longitudinal	Transverse
Lu-Lu	-0.5	-0.5	0	0
Lu-B	2.5	5	4	2
Zr-Zr	0	1	0	0
Zr-B	5.5	0.5	2.3	2

vide important information on the lattice dynamics of MB_{12} compounds in general. The pronounced difference between the equilibrium and phonon-disturbed electron density of states seen in Fig. 5 indicates that Zr vibrations are involved in a sizable electron-phonon coupling. Indeed, the same phonon branch exhibits some softening (Fig. 6) at phonon energies comparable with that of the superconducting gap below T_c . These results suggest a possible role of Zr vibrations in the formation of the superconducting state.

V. CONCLUSION

We have presented the results of a detailed lattice-dynamics study of the ZrB_{12} superconductor using of *ab initio* calculations and inelastic neutron scattering. Similar to rare-earth dodecaborides, the phonon spectrum in ZrB_{12} is mainly determined by the boron sublattice vibrations, and extends up to energies of ~ 140 meV. The low-energy region has a peculiar structure with large weakly dispersive parts in the acoustic phonon branches and a gap between the acoustic and optic branches. Such a shape of the vibration spectrum can be understood in terms of the hierarchy of interatomic interactions, the Zr ions being loosely bound within the rigid boron network, and their vibrations thus having a quasilocal character. The energy of these quasilocal Zr vibration modes was determined to be approximately 17.5 meV. The results of both *ab initio* calculation and INS measurements further indicate that the Zr vibration modes make a appreciable contribution to electron-phonon interactions and may thus take part in the formation of the superconducting state with a rather high-transition temperature $T_c \approx 6$ K.

ACKNOWLEDGMENTS

We are grateful to N. Yu. Shitsevalova, A. S. Ivanov, N. E. Zein, S. Y. Savrasov, G. E. Grechnev, V. V. Glushkov, and V. N. Lazukov for stimulating discussion, and to D. Lamago for his help during the neutron experiment. The financial support of RFBR under Grant No. 08-02-00430 and Russian State under Contract No. 02.740.11.0433 is strongly appreciated.

- *Present address: Jülich Centre for Neutron Science, Forschungszentrum Jülich, Germany.
- ¹H. Kawaji, H. O. Horie, S. Yamanaka, and M. Ishikawa, *Phys. Rev. Lett.* **74**, 1427 (1995).
- ²T. Mori, in *Handbook on the Physics and Chemistry of the Rare Earths*, edited by K. A. Gschneidner, Jr., J. C. Bunzli, and V. Pecharsky (Elsevier, Amsterdam, 2008), Vol. 38, p. 105.
- ³B. T. Matthias, T. H. Geballe, K. Andres, E. Corenzwit, G. W. Hull, and J. P. Maita, *Science* **159**, 530 (1968).
- ⁴Z. Fisk, in *Boron-Rich Solids*, AIP Conf. Proc. No. 231, edited by D. Emin, T. L. Aselage, A. C. Switendick, B. Morosin, and C. L. Beckel (AIP, New York, 1991), p. 155.
- ⁵C. W. Chu and H. H. Hill, *Science* **159**, 1227 (1968).
- ⁶Z. Fisk, A. C. Lawson, B. T. Matthias, and E. Corenzwit, *Phys. Lett. A* **37**, 251 (1971).
- ⁷R. Lortz, Y. Wang, S. Abe, C. Meingast, Yu. B. Paderno, V. Filippov, and A. Junod, *Phys. Rev. B* **72**, 024547 (2005).
- ⁸A. Bouvet, T. Kasuya, M. Bonnet, L. P. Regnault, J. Rossat-Mignod, F. Iga, B. Fåk, and A. Severing, *J. Phys.: Condens. Matter* **10**, 5667 (1998).
- ⁹E. V. Nefedova, P. A. Alekseev, J.-M. Mignot, V. N. Lazukov, I. P. Sadikov, Yu. B. Paderno, N. Yu. Shitsevalova, and R. S. Eccleston, *Phys. Rev. B* **60**, 13507 (1999).
- ¹⁰V. Glushkov, M. Ignatov, S. Demishev, V. Filippov, K. Flachbart, T. Ishchenko, A. Kuznetsov, N. Samarin, N. Shitsevalova, and N. Sluchanko, *Phys. Status Solidi B* **243**, R72 (2006).
- ¹¹H. Werheit, Y. Paderno, V. Filippov, V. Paderno, A. Pietraszko, M. Armbruster, and U. Schwarz, *J. Solid State Chem.* **179**, 2761 (2006).
- ¹²A. V. Rybina, P. A. Alekseev, K. S. Nemkovski, E. V. Nefedova, J.-M. Mignot, Yu. B. Paderno, N. Yu. Shitsevalova, and R. I. Bewley, *Crystallogr. Rep.* **52**, 770 (2007); *Kristallografiya* **52**, 800 (2007).
- ¹³K. S. Nemkovski, P. A. Alekseev, J.-M. Mignot, A. V. Rybina, F. Iga, T. Takabatake, N. Yu. Shitsevalova, Yu. B. Paderno, V. N. Lazukov, E. V. Nefedova, N. N. Tiden, and I. P. Sadikov, *J. Solid State Chem.* **179**, 2895 (2006).
- ¹⁴Yu. B. Paderno, V. Filippov, and N. Shitsevalova, in *Boron-Rich Solids*, AIP Conf. Proc. No. 231, edited by D. Emin, T. L. Aselage, A. C. Switendick, B. Morosin, and C. L. Beckel (AIP, New York, 1991), p. 460.
- ¹⁵G. Kresse and J. Hafner, *Phys. Rev. B* **47**, 558 (1993); **49**, 14251 (1994).
- ¹⁶G. Kresse and J. Furthmuller, *Phys. Rev. B* **54**, 11169 (1996); *Comput. Mater. Sci.* **6**, 15 (1996).
- ¹⁷K. Parlinski, computer code PHONON, Cracow, 2008.
- ¹⁸H. J. Monkhorst and J. D. Pack, *Phys. Rev. B* **13**, 5188 (1976).
- ¹⁹V. A. Gasparov, N. S. Sidorov, and I. I. Zver'kova, *Phys. Rev. B* **73**, 094510 (2006).
- ²⁰G. E. Grechnev, A. E. Baranovskiy, V. D. Fil, T. V. Ignatova, I. G. Kolobov, A. V. Logosha, N. Yu. Shitsevalova, V. B. Filippov, and O. Eriksson, *Low Temp. Phys.* **34**, 921 (2008).
- ²¹P. Elter and G. Eckold, *Physica B* **276-278**, 268 (2000).